JACS
JOURNAL OF THE AMERICAN CHEMICAL SOCIETY

Perspective

pubs.acs.org/JACS

Making Sense of the Mayhem behind Shape Control in the Synthesis of Gold Nanoparticles

Michelle L. Personick and Chad A. Mirkin*

Department of Chemistry and International Institute for Nanotechnology, Northwestern University, 2145 Sheridan Road, Evanston, Illinois 60208, United States

ABSTRACT: The formation of anisotropic Au nanoparticles predominantly follows one of two growth pathways: (1) kinetic control or (2) selective surface passivation. This Perspective describes the mechanisms that control Au nanoparticle shape via these pathways in the context of three basic chemical parameters: metal complex reduction potential, metal ion availability, and adsorbate binding strength. These chemical parameters influence the crystallinity and surface facets of the Au nanoparticles, thus dictating particle shape. Understanding nanoparticle growth mechanisms in terms of simple chemical principles enables mechanistic insights to be more easily applied to other syntheses and gives them greater predictive power in the development of new preparations of metal nanoparticles with well-defined shapes. Background information regarding the growth of Au nanoparticles with control over shape is also provided, along with a perspective on unanswered mechanistic questions in noble-metal nanoparticle synthesis and promising directions for future studies.

1. INTRODUCTION

The field of nanotechnology and the development of novel nanomaterials have been accelerating at a rapid pace in the last few decades as the emergent properties of such materials are discovered and their structure−function relationships are elucidated. The ability to visualize individual nanoparticles, and even atoms, as a result of the development of imaging techniques with nanometer and subnanometer resolution, such as electron microscopy and scanning probe microscopy, has facilitated explanations of the emergent properties of noble-metal nanoparticles, including localized surface plasmon resonance (LSPR), spectroscopic enhancement, and increased catalytic activity, as a consequence of the physical characteristics of the nanoparticles themselves.[1−5] These structure−function relationships are particularly interesting for noble-metal nanoparticles because the properties of such nanostructures are highly dependent not only on material composition but also on size and shape,[1,3,4] which is not the case for the corresponding bulk metal materials. As a result of the key roles of size and shape in directing the physical and chemical properties of noble-metal nanoparticles, it is necessary to rationally and reproducibly tailor these structural parameters in order to optimize the nanoparticles for use in a variety of promising applications, including sensing and spectroscopic enhancement,[3,5−10] catalysis,[1,11−13] energy,[12] and biology.[14] To address this requirement, a vast amount of research has been devoted to the development of a range of methods for producing noble-metal nanoparticles with control over shape and size.[1,7,10,13,15−49] This is especially true in the case of gold.[1,10,25,36,38−46] This Perspective will focus on one such method: the seed-mediated synthesis of Au nanoparticles. In just over 10 years, research regarding the synthesis of Au nanoparticles with control over shape has progressed from serendipitous discoveries to phenomenological observations of trends in nanoparticle formation to a mechanistic understanding of nanoparticle growth. This enhanced understanding of shape-control pathways has enabled the synthesis of novel Au nanoparticle shapes with a variety of surface facets, including {720}-faceted concave cubes,[40] {730}-faceted tetrahexahedra,[42,50] {221}-faceted trisoctahedra,[51,52] {110}-faceted bipyramids,[53] {210}-faceted hexagonal bipyramids,[54] and {111}-faceted octahedra with hollow features (Figure 1).[36] In many cases, each new mechanistic insight that is gained can also be retrospectively applied to further explain a subset of previously reported observations and trends, including some of the earliest published syntheses of metal nanoparticles with

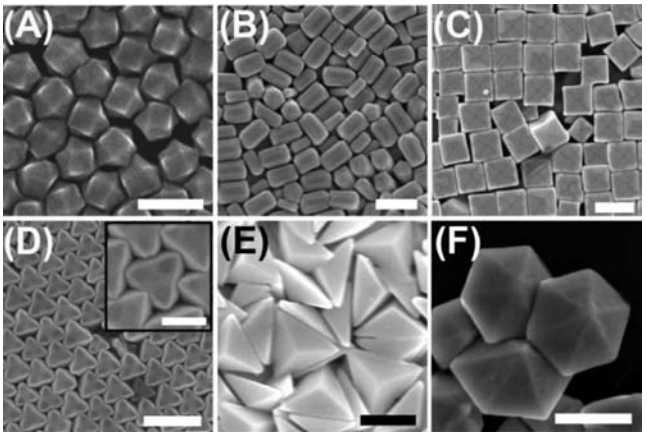

Figure 1. Examples of Au nanoparticles with well-defined shapes and facets: (A) {221}-faceted trisoctahedra;[51,52] (B) {730}-faceted tetrahexahedra;[38,42,50] (C) {720}-faceted concave cubes;[40] (D) {111}-faceted octahedra with tailorable hollow features;[36] (E) {110}-faceted bipyramids;[53] (F) {210}-faceted hexagonal bipyramids.[54] Scale bars: 200 nm. Scale bar in the inset in (D): 50 nm. Adapted with permission from refs (A) 52, (B) 38, (C) 40, (D) 36, (E) 53, and (F) 54. Copyright 2009, 2010, 2011, and 2013 American Chemical Society.

Received: August 20, 2013
Published: November 27, 2013

dx.doi.org/10.1021/ja408645b | J. Am. Chem. Soc. 2013, 135, 18238−18247

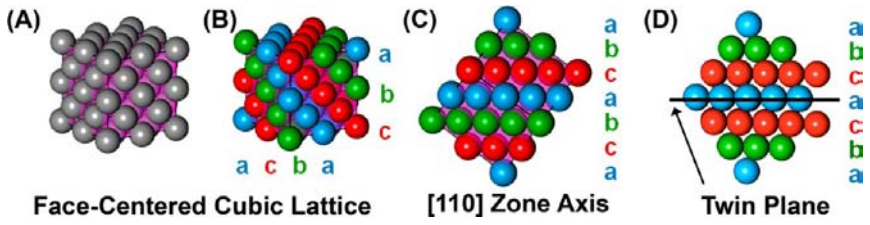

Figure 2. Model of a twin plane in a face-centered cubic (fcc) metal: (A) fcc lattice; (B) fcc lattice with the repeating *abcabcabc* stacking pattern annotated; (C) annotated fcc lattice from (B) oriented to the [110] zone axis so that the {111} repeating layers are more easily visible; (D) annotated fcc lattice which contains a twin plane, as viewed down the [110] zone axis. Here, the insertion of a *c* layer in place of a *b* layer (*abcacba*) in the repeating pattern has resulted in a structure which is mirrored around the central *a* layer (marked with a horizontal line).

well-defined shapes, such as Au nanorods[44,45] and triangular nanoprisms.[6]

In this Perspective, we delineate the mechanisms involved in the major pathways of Au nanoparticle growth—kinetic control and selective surface passivation—in terms of three basic chemical parameters: the reduction potentials of the relevant metal complexes, metal ion concentration, and adsorbate binding strength. In addition, we discuss some important general considerations for probing the chemical and physical factors that control nanoparticle growth. Finally, we provide a perspective on potential future research directions and point out important unanswered questions in the synthesis of Au nanoparticles with control over shape with the goal of inspiring future studies in this highly active research field.

2. STRUCTURE AND MORPHOLOGY OF NOBLE-METAL NANOPARTICLES

Before discussing the details of the synthesis of noble-metal nanoparticles, it is important to first lay out a framework for describing nanoparticle shape and to outline the structural parameters which influence and direct morphology. There are two major structural factors which control nanoparticle shape: surface facets and crystallinity. Of these two characteristics, crystallinity is primarily defined early in particle formation, during the initial nucleation stages, while the establishment of uniform surface facets occurs shortly afterward during the growth of the particle.[1] Specific methods of controlling surface facet structure will be discussed in detail in subsequent sections of this Perspective.

In terms of crystallinity, nanoparticles can be single-crystalline or polycrystalline or may contain a finite number of crystal defects.[1,30,55,56] Single-crystalline and polycrystalline are the extremes, containing zero or many defects, respectively. The most common defects in face-centered cubic (fcc) metals, such as Au and Ag, are twin defects and stacking faults.[55] Stacking faults occur when the *abcabcabc* stacking pattern of layers of metal atoms in the fcc unit cell is disrupted by a missing or added layer: for example, *abcabacabc* (insertion of an *a* layer). When this disruption results in a mirroring of the stacking pattern around one of the layers (i.e. *abcabacba*), a twin plane is formed (Figure 2). This type of defect is common in fcc metals because the coordination number of the atoms in each layer is the same in the perfect crystal as it is when the twin defect is present; therefore, there is a very low energy barrier to the formation of the twin defects in fcc metals.[55] Multiple twin defects can occur in a single nanoparticle, and the most often observed twin structures in Au nanoparticles are planar-twinned (possessing one or more parallel twin defects), penta-twinned (containing five twins which radiate from a central point), and multiply twinned (generally having 20 intersecting twin planes).[1,9] The twin structure of a nanoparticle has a strong influence on determining its symmetry, though the exact shape of the particle is also highly dependent on the structure of its surface (Figure 3).

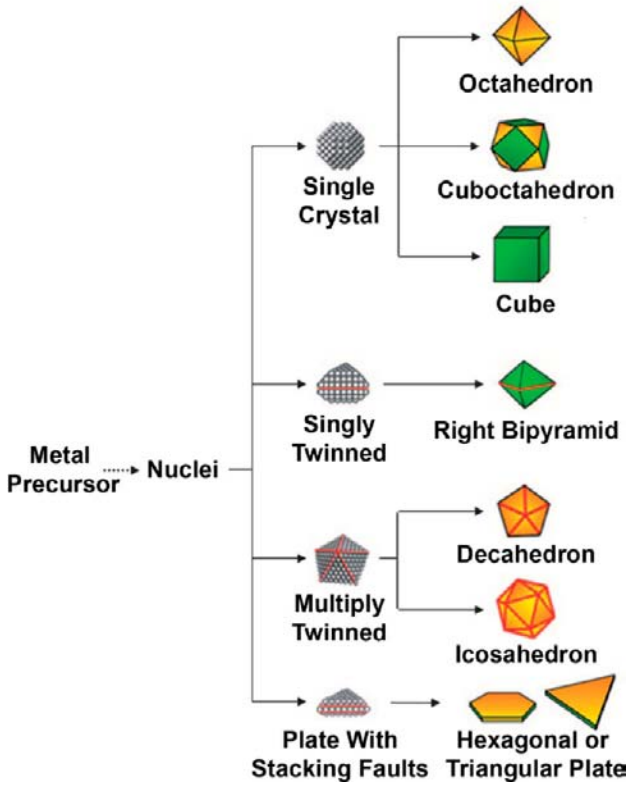

Figure 3. Growth of noble-metal nanoparticles with various twin structures and surface facets. Yellow indicates {111} surface facets, and green represents {100} surface facets. Adapted with permission from ref 1. Copyright 2009 Wiley-VCH.

The faces of polyhedral metal nanocrystals expose surfaces with a particular arrangement of atoms, and these surfaces are referred to as facets. The arrangement of the atoms differs depending on the angle of the exposed surface relative to the overall atomic lattice structure of the metal unit cell. As a result, these facets can be described by a set of integers, known as Miller indices, which indicate the orientation of the plane of the facet with respect to the unit cell. For example, cubes are bound by {100} surface facets, the plane of which lies along a face of an fcc unit cell (Figure 4). Facets where all of the integers in the Miller index are either 1 or 0, {111}, {100}, and {110}, are referred to as low-index facets and represent the lowest-energy

dx.doi.org/10.1021/ja408645b | J. Am. Chem. Soc. 2013, 135, 18238−18247

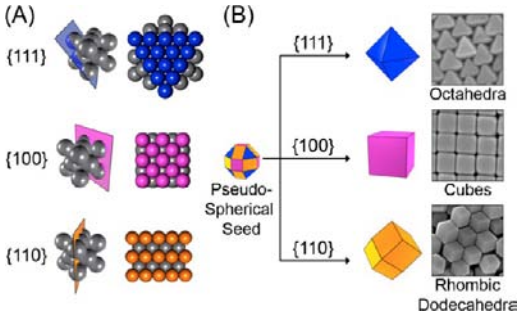

Figure 4. (A) Models of the low-index surface facets of fcc metals, such as Au. (B) Models (left) and scanning electron microscopy (SEM) images (right) of representative polyhedral nanoparticle shapes bound by each of the low-index facets.

surfaces for fcc nanoparticles.[57] Examples of polyhedral nanoparticle shapes bound by {111} and {110} facets are octahedra and rhombic dodecahedra, respectively (Figure 4). Of the three low-index facets, {111} facets, which have a close-packed arrangement of atoms, are the most thermodynamically favored facets for an fcc metal.[57] Many different methods exist for selectively favoring the growth of particles bound by particular facets, including kinetic control, selective surface passivation by ions and small molecules, and physical templating.[1,9,10] This Perspective will focus on chemical control of surface structure in aqueous seed-mediated syntheses of Au nanoparticles, which are perhaps the most versatile solution-based methods for producing Au nanoparticles with control over shape.

3. OVERVIEW OF SEED-MEDIATED SYNTHESES OF AU NANOPARTICLES

Seed-mediated syntheses of Au nanoparticles have been used to achieve the growth of an extensive library of nanoparticle shapes, including simple polyhedra such as Platonic solids (for example, cubes and octahedra),[27,46,58−60] as well as prisms and plates,[6,7,61,62] and more exotic structures with high-index facets and concave surfaces.[39,40,42,52,54,63,64] The seed-mediated synthesis of Au particles can be divided into two main synthetic steps: (1) the rapid reduction of Au ions to form small, highly monodisperse spherical Au nanoparticles, or seeds, and (2) the growth of larger nanoparticles by slowly reducing additional Au onto the previously synthesized seeds (which serve as nucleation sites) in the presence of shape-directing additives (Figure 5).[65,66] In this way, the nucleation and growth phases of nanoparticle formation are temporally separated, which helps ensure monodispersity in the final nanoparticle colloid. Seeded growth also enables size control through adjustments of the ratio between the seed and Au ion concentrations. The addition of more seeds leads to more, but smaller, particles for a constant Au ion concentration, while the addition of fewer seeds generates fewer, but larger, particles.

The first step—the formation of the seed particles—is largely the same across all of the reported seed-mediated syntheses. Seed particles are synthesized via the reduction of tetrachloroauric acid ($HAuCl_4$) by a strong reducing agent, usually sodium borohyride ($NaBH_4$) in the presence of a stabilizing agent, commonly the surfactant cetyltrimethylammonium bromide (CTAB), though cetylrimethylammonium chloride (CTAC) and sodium citrate have also been used.[40,45,61,63,65] While sodium citrate is not a surfactant, it can serve to stabilize the nanoparticles by binding to the particle surface and thus providing an overall negative surface charge which prevents aggregation. The use of a strong reducing agent in the seed formation process ensures that the particles which result are small and monodisperse, due to the simultaneous rapid nucleation of a large number of nanoparticles in the solution. The seeds that form are generally about 3−7 nm, with some variation in their average size depending on the exact conditions and surfactant used in their synthesis.[63] The choice of surfactant or stabilizing agent can also affect the crystallinity of the seeds, with sodium citrate leading to primarily multiply twinned and planar-twinned seeds, while the use of CTAB results in a population of seeds which is largely single-crystalline.[63] The reason for this difference in crystallinity is generally attributed to differences in reaction kinetics.[1,67] More recently, Xu et al. have also reported a procedure for synthesizing larger (~40 nm) single-crystalline seeds by first growing single-crystalline Au nanorods and then transforming the rods into spherical nanoparticles via a multistep process of overgrowth and etching.[27] These spheres are subsequently used to seed the growth of single-crystalline nanoparticles which have other shapes, such as octahedra, rhombic dodecahedra, and cubes.[27]

The high degree of shape control and tailorability that is characteristic of seed-mediated syntheses of Au nanoparticles is primarily achieved in the second growth step. In this step, the seed particles are added to a reaction solution, known in the nanoparticle synthesis literature as a growth solution, which contains at minimum a surfactant, a source of Au ions, and a weak reducing agent.[45,65] In this second growth step, a weak reducing agent is chosen to prevent additional nucleation and

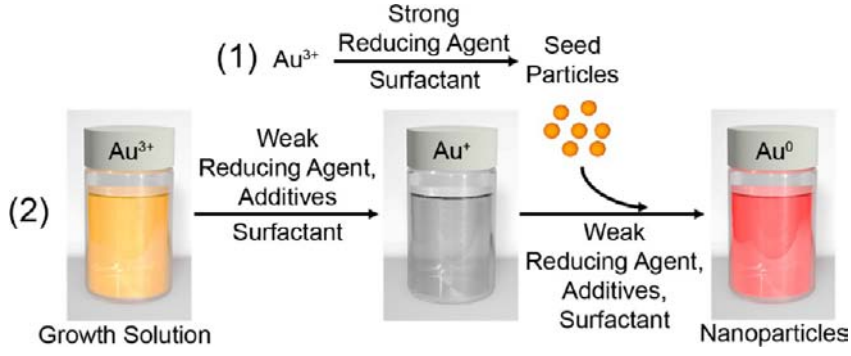

Figure 5. Simplified schematic representation of the two steps of the seed-mediated synthesis of Au nanoparticles: (1) rapid reduction of Au^{3+} to Au^0 form small seed particles; (2) slow, controlled deposition of Au onto the preformed seeds in the presence of shape-directing additives.

dx.doi.org/10.1021/ja408645b | J. Am. Chem. Soc. 2013, 135, 18238−18247

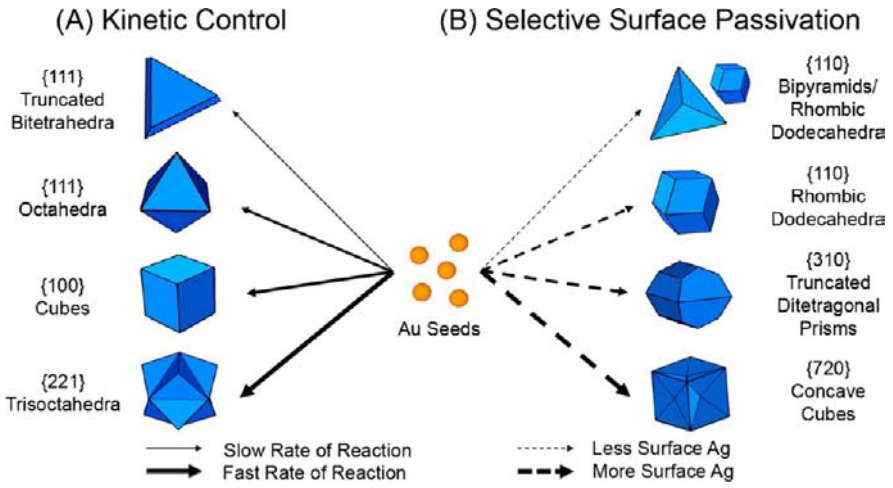

Figure 6. Schematic representation of the two primary growth pathways of Au nanoparticles: (A) kinetic control; (B) selective surface passivation (in this case, by Ag). Under kinetic control, the rate of Au^+ reduction directs nanoparticle shape. In the selective surface passivation pathway, the deposition of Ag onto the Au nanoparticle surface blocks the growth of particular facets and thus dictates nanoparticle shape. Adapted with permission from ref 38. Copyright 2012 American Chemical Society.

to favor growth onto the preformed seeds, as well as to slow particle growth enough to allow for control of nanoparticle shape through the addition of shape-directing additives. Ascorbic acid is most commonly used as the reducing agent because it is weaker than $NaBH_4$, and also because the reducing ability of ascorbic acid can be easily tuned through adjustment of the solution pH, decreasing in strength at lower pH values. Reduction of Au^{3+} to Au^+ by ascorbic acid is rapid, but the subsequent reduction of Au^+ to Au^0 at low pH is very slow and is negligible in the absence of the seed particles, which serve to catalyze the second reduction step.[65] If $NaBH_4$ were again used as the reducing agent in this step, the result would be the formation of additional small Au nuclei, rather than the desired growth of larger nanoparticles with anisotropic shapes. With the seed-mediated approach, a wide variety of shapes can be achieved through the addition of shape-directing additives, most commonly Ag ions and halide ions. However, while seed-mediated syntheses have been widely used to produce uniform solutions of popular Au nanoparticle shapes, especially rods,[44,45] triangular nanoprisms,[6,61,62] cubes,[27,46,68] and octahedra,[27] the mechanistic explanations for why the syntheses yield particular shapes have often lagged behind the optimization of the synthetic methods, and only recently has a coherent mechanistic understanding of Au nanoparticle growth begun to emerge in the literature.[1,27,38,39,60,63,68]

4. KINETIC CONTROL AND SELECTIVE SURFACE PASSIVATION: TWO DIFFERENT GROWTH PATHWAYS GUIDED BY SIMILAR CHEMISTRY

The mechanisms of metal nanocrystal shape control, particularly those pertaining to the seed-mediated synthesis of Au nanoparticles, can be divided into two primary growth pathways: kinetic control and selective surface passivation (Figure 6).[1,38] Under the kinetic control pathway, nanoparticle shape is directed by the overall rate of metal ion reduction (reduction of Au^+ in the case of Au nanoparticles).[1,38,60,69] Slower rates of Au^+ reduction generally lead to more thermodynamically favored shapes with low-index facets, such as {111}-faceted octahedra, while faster rates of Au^+ reduction result in the formation of kinetic products, such as high-index {221}-faceted trisoctahedra.[38,60] In contrast, the selective passivation of a particular surface facet by a bound adsorbate (such as Ag in the Ag-assisted synthesis of Au nanoparticles) controls nanoparticle formation by slowing the growth of one type of facet relative to the growth of other facets.[38,39,45,63] Au deposits more rapidly on the unpassivated surfaces, causing them to grow until they develop the same facet structure as the passivated surface, and this results in a particle bound entirely by the passivated facet. While these two growth pathways at first appear to be mechanistically divergent, the factors which direct nanoparticle growth in both cases are derived from the synergistic effects of the same three basic chemistry principles: the reduction potential of the metal complexes, metal ion availability, and adsorbate binding strength.

Kinetic Pathway. In the case of the kinetically controlled growth pathway, each of these three basic chemical principles plays an influential role in moderating the rate of Au^+ reduction. For example, the reduction potential of Au^+ is strongly affected by the presence of the halides chloride, bromide, and iodide in the growth solution, and this change in reduction potential can modulate the rate of Au^+ reduction. Of these three anions, the presence of chloride results in an Au–halide complex with the highest relative reduction potential, and thus the Au–halide complex which is most easily reduced, while the presence of bromide or iodide leads to Au complexes with lower reduction potentials, with Au–iodide complexes being the most difficult to reduce.[70] Thus, given a constant concentration of reducing agent, the addition of a larger halide ($Cl^- < Br^- < I^-$) will slow the rate of Au^+ reduction, with iodide having a much more drastic slowing effect than bromide at a similar concentration of halide ion.[38] This slowed reduction rate as a result of changes in the reduction potential of the Au complex can be compensated for or counterbalanced by the addition of a greater excess of ascorbic acid or by raising the pH of the growth solution to increase the reducing strength of the ascorbic acid, both of which will speed the rate of Au^+ reduction.[38,52,60,68,69] Together, this balance between the reduction potential of the Au complex and the strength of the reducing agent is a major contributor to determining the kinetics of Au^+ reduction.

However, reduction potential is not the only factor in dictating the kinetics of nanoparticle growth. Indeed, metal ion

dx.doi.org/10.1021/ja408645b | J. Am. Chem. Soc. 2013, 135, 18238–18247

availability will also influence the Au^+ reduction rate by changing the effective concentration of Au^+ in solution and, consequently, the amount of Au^+ available for reduction. The solubilities of the Au−halide complexes decrease in the order $[AuCl_2]^- > [AuBr_2]^- > [AuI_2]^-$,[71] resulting in a decrease in the equilibrium concentration of Au^+ in solution and a corresponding decrease in the rate of Au^+ reduction in that same order.[38] Adsorbate binding strength also changes the rate of Au^+ reduction by modulating the amount of surface area on the growing Au nanoparticles that is available to catalyze the reduction of Au^+ to Au^0. The relative binding strength of the halides to the Au nanoparticle surface increases in the order $Cl^- < Br^- < I^-$.[72] As the binding strength of the halide to Au increases, the desorption of the halide from the Au nanoparticle surface becomes less facile and there is less Au surface area available at any given time to facilitate the reduction of Au^+; therefore, Au^+ reduction is slowed.[38]

By considering the combined influences of these three basic chemical parameters: reduction potential, metal ion availability, and adsorbate binding strength, it is possible to qualitatively predict the effect that a particular additive will have on the rate of Au^+ reduction and thus also to deliberately shift the kinetics of nanoparticle growth to favor a particular morphology under the kinetic growth pathway through the judicious control of additive concentration. For example, in the case of halide ions, the overall result of these three parameters is that the addition of increasing concentrations of a larger halide ion progressively slows the rate of Au^+ reduction, thus favoring nanoparticle shapes with increasingly low-energy surfaces (Figure 6A), with iodide having a stronger effect on reaction rate than bromide does.[38] While reduction potential might initially seem to be the most straightforward contributor to kinetic control from among the three chemical parameters, it is ultimately necessary to consider all three together. Likewise, in the case of shape control by selective surface passivation, it is not only adsorbate binding strength which is influential in controlling growth but also the reduction potential and availability of the metal complexes and ions. In the following section, the synergistic roles of each of the three chemical parameters are discussed in the context of the Ag underpotential deposition (UPD) controlled growth of Au nanostructures (also known as Ag-assisted growth).

Selective Surface Passivation Pathway. In the Ag UPD controlled growth of Au nanostructures, the surface facets of the nanoparticles and, consequently, their shapes, are dictated by the amount of Ag that is deposited onto the surface of the Au particle during the growth process.[38,39] This method is an example of growth via the selective surface passivation pathway. Detailed mechanistic studies have shown that, as more Ag is deposited onto the growing Au nanoparticle, increasingly more open facets, which expose greater numbers of surface atoms, are passivated and stabilized (Figures 6B and 7).[38,39] These open surface facets are often high-index, and this method has led to the preparation of a number of novel high-index nanostructures, such as tetrahexahedra and concave cubes.[40,42] The amount of Ag which is reduced onto the surface of the Au nanoparticles via UPD is correlated with the concentration of Ag^+ in the growth solution and modulated by the three basic chemical parameters of nanoparticle growth described above (Figure 7).[38,39] First, it is as a consequence of the reduction potential of the metal ions relative to the strength of the reducing agent (ascorbic acid) that UPD of Ag on Au takes place in this system. Ag UPD on Au is defined as the reduction

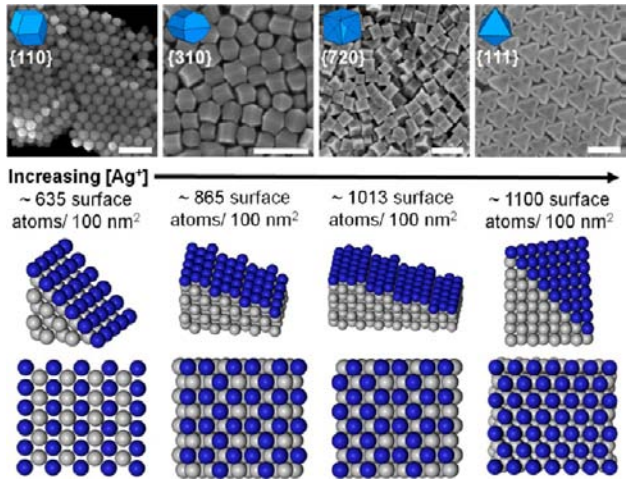

Figure 7. SEM images and models of various nanoparticle shapes (top) and models of their respective surface facets (bottom), illustrating the relationship between Ag^+ concentration and facet passivation. Shapes from left to right: {110}-faceted rhombic dodecahedra, {310}-faceted truncated ditetragonal prisms, {720}-faceted concave cubes, and {111}-faceted octahedra with hollow cavities. Scale bars: 200 nm. Higher concentrations of Ag^+ lead to the stabilization of facets with a progressively greater number of exposed surface atoms. Adapted with permission from refs 36 and 39. Copyright 2011 American Chemical Society.

of up to a monolayer of Ag onto an existing Au surface at a potential positive to the Nernst potential of Ag.[63,73,74] In the case of Au nanoparticle syntheses, this deposition in the underpotential regime becomes relevant because ascorbic acid is not a strong enough reducing agent to reduce Ag^+ at the low pH conditions generally employed with these synthetic approaches (pH ~2).[39,63,74] Despite this mismatch between the strength of the reducing agent and the reduction potential of Ag^+, up to a monolayer of Ag can still be deposited onto the growing Au nanoparticles when facilitated by the surface of the nanoparticles.[39,63,74] The second basic chemistry parameter, metal ion availability, can impact this UPD process when halide ions are present in solution along with the Ag^+ ions and the growing Au nanoparticles. The solubility of the Ag−halide complexes decreases in the order AgCl > AgBr > AgI,[71] and the lower solubility diminishes the amount of Ag^+ available for reduction, thus slowing Ag deposition and leading to a lower coverage of Ag on the Au nanoparticle surface and the stabilization of less open facets.[38] Halide ions also affect the binding strength of the adsorbed Ag (Ag_{UPD}), and the consequences of this will be discussed later.

The binding strength of Ag to the Au surface is, of course, very important in Ag UPD controlled growth processes. In accordance with surface chemistry studies of Ag UPD, Ag preferentially binds to Au facets which possess more exposed surface atoms, since these surface atoms provide a high coordination number, and thus enhanced stability, for the deposited Ag atoms.[39,63,75,76] As a result, underpotentially deposited Ag selectively passivates facets with as many exposed surface atoms as possible, on the basis of the concentration of Ag^+ in solution, the rate at which Ag can be deposited on the surface (as discussed in the previous paragraph), and the stability of the Ag_{UPD} adlayer.[38,39] If there is not sufficient Ag on the nanoparticle surface to completely passivate a particular facet, that facet will continue to grow despite the presence of Ag on the surface, and the Ag will ultimately stabilize a less

open facet which it can more fully passivate.[39] The binding of Ag to the Au surface in Ag UPD controlled growth reactions does affect the overall kinetics of Au^+ reduction and results in a very slow rate of Au^+ reduction at all Ag^+ concentrations (Figure 8), because the Ag on the nanoparticle surface limits

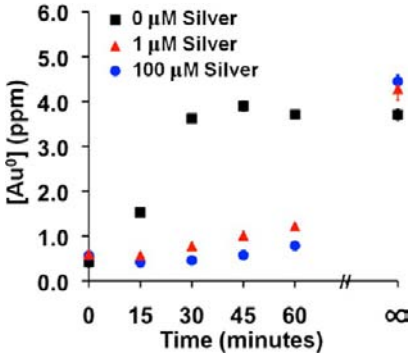

Figure 8. Graph of the rate of Au nanoparticle formation in the presence of 0 μM Ag^+ (black squares), 1 μM Ag^+ (red triangles), and 100 μM Ag^+ (blue circles), as measured by the increase in Au^0 concentration (quantified by inductively coupled plasma atomic emission spectroscopy (ICP-AES)).[38] The addition of a small amount of Ag^+ (1 μM) significantly slows nanoparticle formation, leading to the growth of thermodynamically favored {111}-faceted octahedra. The difference in reaction rate between 1 μM Ag^+ and 100 μM Ag^+ (the conditions under which Ag UPD stabilized concave cubes form) is not significant enough for kinetics to be solely responsible for shape control. Adapted with permission from ref 38. Copyright 2012 American Chemical Society.

the amount of Au surface area that is available to catalyze the reduction of Au^+. Even under conditions where there is not enough Ag being deposited to fully stabilize a particular facet, thermodynamically favored {111}-faceted nanoparticles, such as octahedra, form via a kinetic growth pathway simply as a result of the slow rate of Au^+ reduction.[38,39] However, it is important to note that all of the Ag-assisted growth reactions exhibit comparably slow rates of Au^+ reduction, and the difference in reaction rate at different Ag^+ concentrations is not significant enough to be solely responsible for shape control (Figure 8).[38] Thus, at higher surface coverages of Ag, selective surface passivation becomes dominant over kinetically controlled growth.

In addition to considerations of maximizing the binding strength of Ag to Au through strong coordination to the surface, the introduction of halide ions can also greatly impact the binding of the Ag_{UPD} adsorbate to the Au nanoparticles as a result of the different strengths of the binding interactions of the halide ions with Ag and Au surfaces. Chloride, for example, binds to Ag and Au surfaces with approximately equal strength and thus does not compete significantly with Ag for binding to the Au surface.[75] This results in an Ag_{UPD} layer which possesses an enhanced stability in comparison to an Ag_{UPD} layer deposited in the presence of any other halide ion.[75−77] In the presence of chloride, a high coverage of Ag is rapidly reduced onto the Au nanoparticle surface and stabilized by chloride, making the Ag difficult to displace or rearrange except through slow oxidative dissolution and rereduction. The consequence of this stability for the growth of Au nanoparticles is that a wider variety of shapes can be produced in a chloride-containing surfactant than in a bromide-containing surfactant or in the presence of high concentrations of iodide.[38] This added stability also enables the formation of concave cubes by establishing the concave structure from an early growth stage, maintaining the smaller center portion of the concave cube, and preventing rearrangement to form a convex nanostructure.[38,40]

In contrast, both bromide and iodide bind very strongly to Au surfaces and, as a result, these ions compete with Ag for binding sites, thus blocking and displacing Ag and destabilizing the Ag_{UPD} layer.[73,75,78] This destabilization of the Ag_{UPD} layer in the presence of bromide or iodide relative to the stability of the Ag_{UPD} layer in the presence of chloride fits well with measurements from the bulk surface chemistry literature regarding the stripping potentials of Ag_{UPD} under each of these conditions and in the absence of halides.[78] The stripping peaks are 615, 574, and 415 mV in the presence of chloride, bromide, and iodide, respectively, and 534 mV in the absence of halides (in the presence of sulfate ions).[78] However, this destabilizing effect of halide adsorbates on the binding strength of the adsorbed Ag must be carefully considered within the context of the specific nanoparticle growth conditions, as destabilization results in two different changes to the Ag_{UPD} layer and consequently to particle shape, depending on the concentration of bromide in solution. At high bromide concentrations ($[Br^-] > [Au^+]$), destabilization of the Ag_{UPD} layer results in less Ag on the nanoparticle surface, as might be predicted on the basis of the competition of bromide with Ag for surface binding.[38] However, at low bromide concentrations ($[Br^-] < [Au^+]$), the destabilizing effect is much less drastic and, rather than inhibiting Ag deposition, bromide causes the Ag_{UPD} layer to become slightly more mobile, allowing the Ag to rearrange to more energetically favorable surface sites.[38] This enables more Ag to deposit on the Au nanoparticle surface in comparison to the Ag coverage observed in the presence of chloride.[38] These conditions lead to the formation of higher-index nanostructures at solution concentrations of Ag^+ which are lower than what would be required in the absence of bromide.[38] As phenomenological observations, these two results would perhaps seem contradictory, but they are easily reconciled under this overarching mechanistic understanding. Together, the relative reduction potentials of Ag^+ and Au^+ with respect to each other and to the reduction potential of ascorbic acid, the solubility of the Ag ions in the presence of different halides, and the relative binding strengths of the Ag and halide adsorbates serve to regulate the passivation of the Au nanoparticle surface by Ag_{UPD}, thus guiding particle formation. Overall, when considering the above mechanisms, it is apparent that it is important not only to take into account the particular shape-directing additive being studied but also to consider the other chemical components of the system, as well as what the primary pathway of shape control is in the particular synthesis: i.e., kinetic control or surface passivation.

5. IMPORTANCE OF DISTINGUISHING BETWEEN KINETIC CONTROL AND SELECTIVE SURFACE PASSIVATION

By considering the effects of various shape-directing additives on nanoparticle growth in the context of the same three overarching basic chemistry principles, the relative strengths of the effects of each additive can be evaluated, and this information can then be used to determine the dominant pathway of nanoparticle growth in a particular synthesis. An illustrative example of the importance of considering the dominant shape control pathway is the use of bromide as a shape-directing additive. In a kinetic growth pathway, the role

of bromide is primarily to control the rate of Au^+ reduction, while in the selective surface passivation pathway (using Ag), bromide controls the shape by influencing the stability of the underpotentially deposited Ag adlayer.[38] The difference occurs because all of the Au nanoparticle growth reactions which take place in the presence of Ag^+ are very slow, as shown using ICP-AES (Figure 8) and visibly manifested in the formation of thermodynamically favored octahedra at very low concentrations of Ag^+.[38,39] It is important to consider the relative magnitudes of the kinetic effects caused by Ag^+ and bromide, and in this case, the effect of added bromide on the rate of Au^+ reduction is negligible compared to that of added Ag^+. This mechanistic distinction explains a set of seemingly contradictory observations regarding the effect of bromide on the rate of Au nanoparticle growth. In the absence of Ag^+, the addition of bromide slows particle growth, while in the presence of Ag^+, the addition of bromide increases the rate of particle growth.[38] The reason for these opposite trends is that, in the absence of Ag^+, the dominant role of bromide is to control the rate of Au^+ reduction by changing the reduction potential of Au^+ and by binding to the Au nanoparticle surface, while in the presence of Ag^+, the destabilization of the Ag_{UPD} layer caused by bromide makes the surface of the Au nanoparticle more readily accessible for the catalysis of Au^+ reduction and subsequent Au deposition, thereby increasing the rate of nanoparticle growth.[38]

Differentiation between the kinetic and surface passivation effects of bromide also can be used to understand other existing results, for example, a previously reported study where in the absence of Ag^+ the concentration of bromide was held constant while the ascorbic acid concentration was varied, resulting in a sequence of shapes ranging from truncated cubes to rhombic dodecahedra (Figure 9).[68] To explain early syntheses of Au cubes, which were synthesized in a bromide-containing surfactant (CTAB), it was proposed that bromide ions or CTAB molecules adsorb selectively to {100} facets, stabilizing them and leading to the exclusive formation of cubes.[27,46,52] However, the example above, along with other related cases from the literature,[60] seems contrary to this explanation, as multiple different particle shapes are produced in the presence of bromide through very slight variations in the concentration of the ascorbic acid reducing agent. This discrepancy can be explained by understanding that the kinetic effects of bromide and ascorbic acid on the reduction rate of Au^+ have similar magnitudes, and thus ascorbic acid and bromide can both synergistically control the reaction rate in this system. The authors of the more recent work report that the presence of bromide is necessary for the formation of the various shapes.[68] Taking into account this requirement and the kinetic growth pathway described in this Perspective, it is likely that bromide initially slows Au^+ reduction to a suitable rate for shape control to occur, while minor increases in the concentration of ascorbic acid slightly increase the rate of Au^+ reduction and nanoparticle growth, thus enabling the selective formation of the different shapes. Further, it can be seen that, in this case, the effect of ascorbic acid on the kinetics of the reaction is more significant in directing nanoparticle shape than any facet-specific surface binding effects of bromide or CTAB. The literature regarding the synthesis of metal nanoparticles with defined shapes contains many such observations and claims, which are seemingly contradictory, and the mechanisms put forth in the preceding sections of this Perspective represent a significant step toward explaining a number of them by providing a set of unifying basic chemistry parameters with which to approach nanoparticle growth.

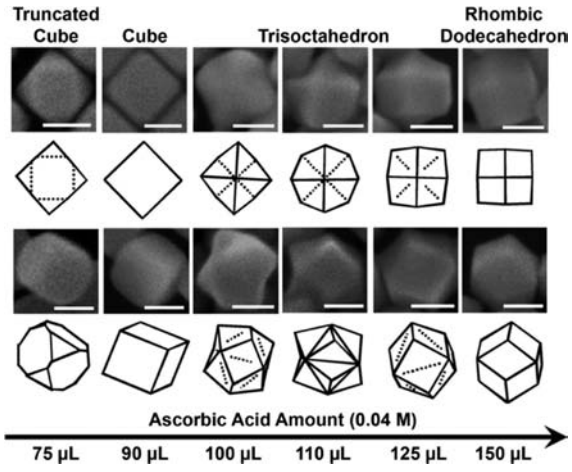

Figure 9. SEM images of the evolution of Au nanoparticle shapes from truncated cube to rhombic dodecahedron as a result of an increasing concentration of ascorbic acid in the nanoparticle growth solution. Shapes without name labels are transitional products. Scale bars: 50 nm. Adapted with permission from ref 68. Copyright 2010 American Chemical Society.

6. OUTLOOK

Importantly, the mechanistic understanding that has been put forth in the recent literature also informs future studies and provides a base of knowledge from which to approach new, complex questions in noble-metal nanoparticle synthesis. The most direct contribution of this work to future studies is in the optimization of existing, and potentially future, syntheses for nanoparticles with different shapes. Noble-metal nanoparticle synthesis is notoriously sensitive to batch-to-batch differences in surfactants and other reagents. By understanding the roles of different additives, it is possible to take the nanoparticle product achieved in a specific laboratory situation and rationally optimize the synthetic conditions to achieve the desired product by compensating for changes caused by different batches of chemicals and other contributing factors, such as minor variations in synthetic technique. For example, in the case of shapes synthesized via kinetic control, the reaction rate can be deliberately adjusted using ascorbic acid or halides to achieve the intended shape and yield of products if the published conditions do not work exactly as originally reported when using chemicals from a batch or manufacturer different from those used in the original work. This concept was previously shown in the specific case of Au triangular nanoprisms, where the formation of nanoprisms exhibits a strong dependence on trace concentrations of iodide in particular batches of CTAB and, to resolve this issue, iodide could be added to ultrapure CTAB at appropriate concentrations to achieve consistently high yields of the nanoprisms.[62] Understanding kinetic control is also necessary to compensate for the use of different sizes of seed particles in seed-mediated syntheses, as larger seeds are less reactive than smaller seeds. Thus, the use of larger seeds generally requires the addition of a higher concentration of reducing agent to achieve the same shape as would be generated from small seeds under the given conditions, and vice versa. Further, in the case of reactions controlled by Ag UPD, differences in the quality of the product

nanoparticles as a result of variations in the halide concentration in a given batch of surfactant can be corrected through the addition of halide ions to the different surfactants, in consultation with the design parameters set forth in this Perspective and in the literature.[38]

With respect to new directions of exploration, mechanistic studies often raise additional questions, and the work discussed here is no exception. A number of these questions relate to the growth of concave cubes and tetrahexahedra, which form under identical synthetic conditions except for the use of the chloride-containing surfactant CTAC in the former case and the bromide-containing surfactant CTAB in the latter case.[40,42] Concave shapes are not likely to form in the presence of high concentrations of bromide, because the destabilized Ag_{UPD} layer in the presence of bromide makes maintaining a concave structure throughout particle growth difficult.[38] However, what exactly drives the formation of concave structures in CTAC under these conditions when a convex structure might be more energetically favorable is still unknown. Another difficult unanswered question is why symmetry breaking occurs in single-crystalline tetrahexahedra, leading to rodlike structures rather than symmetric cubic structures.[42] This question also applies to the growth of single-crystalline Au nanorods,[45] as well as to concave cubes, which develop an aspect ratio of slightly greater than 1 when they are synthesized at very small sizes.[40] In addition, it has been shown that tetrahexahedra are stabilized by only 37−47% of a monolayer of Ag on their surface due to destabilization of the Ag adlayer by bromide, while shapes synthesized in CTAC possess a much higher Ag coverage (~80%).[38] One explanation for why tetrahexahedra can still be stabilized with such a low coverage of Ag is that Ag binds to high-energy, low-coordinate sites on the Au surface, such as step edges, the stabilization of which is a key to preserving high-index facets.[38] However, this observation might benefit from further exploration into why the tetrahexahedral shape is preferentially stabilized over another shape with fewer surface atoms. Probing the coordination of the Ag atoms on the surface of the tetrahexahedra and other shapes using techniques such as extended X-ray absorption fine structure (EXAFS) may lend insight into whether the Ag atoms are in fact located primarily at step edges, and this information could be compared to the data collected from other Ag UPD controlled shapes. It is also possible that there is some innate stability to the tetrahexahedral morphology, which has a large number of smaller facets and therefore has surface characteristics that are geometrically reminiscent of a sphere, which is a very stable shape.

Investigations of factors which specifically influence nanoparticle twin structure also open up areas of further study. In the synthesis of {110}-faceted bipyramids and rhombic dodecahedra, the use of a lower CTAC concentration (40 mM) coupled with the addition of sodium chloride (to keep the total chloride concentration constant at 100 mM) results in the formation of a higher quality planar-twinned bipyramidal product than does the use of 100 mM CTAC, which favors the formation of larger rhombic dodecahedra and more truncated bipyramids (Figure 10).[53] While this effect has not been studied in detail, one possibility is that the surfactant binds to the re-entrant grooves which result from the presence of twin planes in the equatorial region of the twinned bipyramids, preventing the bipyramids from growing out as rapidly in the lateral direction and, consequently, leading to truncation. Another possible origin of this difference is that the concentration of surfactant affects the concentration of available Au^+, and thus the rate of particle growth, through complexation of Au^+ by CTAC molecules or incorporation of Au^+ into CTAC micelles.[79,80] This influence of surfactant concentration on the relative growth rates of nanoparticles with different twin structures may be interesting to investigate further.

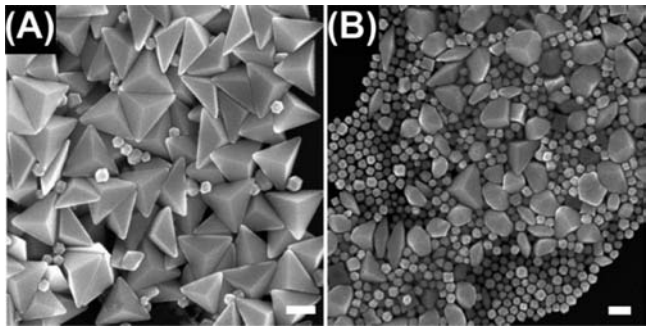

Figure 10. SEM images of {110}-faceted bipyramids and rhombic dodecahedra synthesized in (A) 40 mM CTAC and (B) 100 mM CTAC. Scale bars: 200 nm. Higher quality twinned bipyramids are formed in 40 mM CTAC in comparison to those in 100 mM CTAC. Image in (A) reproduced with permission from ref 53. Copyright 2011 American Chemical Society.

It is hoped that the mechanisms discussed herein will also serve to inspire and guide studies involving other synthetic systems for producing nanoparticles with well-defined shapes, including the syntheses of nanoparticles composed of other metals as well as the potential use of other UPD pairs such as Cu or Pb UPD on Au[73,81] or Cu UPD on Pd[82] to control nanoparticle shape. Indeed, the mechanisms governing the kinetic influences of halides on the rate of metal ion reduction, as described in this Perspective, have very recently been shown by Xia and co-workers to be applicable in the case of Pd nanoparticles as well, with increasing concentrations of bromide resulting in slower reduction of Pd^{2+} and thus the formation of Pd nanoparticles with different shapes.[83] The shapes match those formed in the case of Au nanoparticles in the presence of bromide and iodide ions and range from truncated cubes at low concentrations of bromide to cubes and octahedra at increasing concentrations of bromide to a mixture of truncated bitetrahedra and octahedra at the highest bromide ion concentrations.[38,84] With respect to the other metal UPD systems mentioned above, the relative lattice parameters of these other metals have greater mismatches than do Ag and Au, and the differences in their reduction potentials have varying magnitudes, both of which will likely require the use of conditions which differ from those employed for Ag UPD on Au, such as the use of a reducing agent other than ascorbic acid. However, the mechanisms outlined in this Perspective can provide some guidance for the development of conditions for harnessing these other UPD pairs as surface passivation agents to control noble-metal nanoparticle shape.

7. CONCLUSIONS

Together, the mechanisms discussed in this Perspective, along with work set forth in the recent literature, significantly advance the field of metal nanoparticle synthesis not only through the elucidation of new design parameters for controlling nanoparticle shape and through the development of syntheses for nanoparticles with novel shapes, but also by providing mechanistic insight into previously reported syntheses and by

opening up pathways for future studies of complex questions. Most importantly, this Perspective lays out a unifying framework for exploring these questions by using well-understood concepts from chemistry as tools to unravel the seeming mayhem behind the shape control of Au nanoparticles. These mechanisms and tools, which are derived from very basic and universal chemical principles, also potentially can be applied to nanoparticle preparations involving other solution-based synthetic methods and different nanoparticle compositions and will thereby make a continuing contribution to noble-metal nanoparticle synthesis.

AUTHOR INFORMATION

Corresponding Author

chadnano@northwestern.edu

Notes

The authors declare no competing financial interest.

ACKNOWLEDGMENTS

This work was supported by AFOSR Awards FA9550-11-1-0275, FA9550-12-1-0280, and FA9550-09-1-0294, DoD/NSSEFF/NPS Award N00244-09-1-0012, the NU Nonequilibrium Energy Research Center (NERC) DOE Award DE-SC0000989, Nanoscale Science and Engineering Initiative NSF Award EEC-0647560, NSF MRSEC (DMR-0520513 and DMR-1121262), and shared Facilities at the Materials Research Center. M.L.P. gratefully acknowledges support from the NSF through a Graduate Research Fellowship and from the DoD through the National Defense Science & Engineering Graduate (NDSEG) Fellowship Program (32 CFR 168a).

REFERENCES

(1) Xia, Y.; Xiong, Y.; Lim, B.; Skrabalak, S. E. *Angew. Chem., Int. Ed.* **2009**, *48*, 60.
(2) Aherne, D.; Ledwith, D. M.; Gara, M.; Kelly, J. M. *Adv. Funct. Mater.* **2008**, *18*, 2005.
(3) Kelly, K. L.; Coronado, E.; Zhao, L. L.; Schatz, G. C. *J. Phys. Chem. B* **2003**, *107*, 668.
(4) Sau, T. K.; Rogach, A. L.; Jäckel, F.; Klar, T. A.; Feldmann, J. *Adv. Mater.* **2010**, *22*, 1805.
(5) Rycenga, M.; Cobley, C. M.; Zeng, J.; Li, W.; Moran, C. H.; Zhang, Q.; Qin, D.; Xia, Y. *Chem. Rev.* **2011**, *111*, 3669.
(6) Millstone, J. E.; Park, S.; Shuford, K. L.; Qin, L.; Schatz, G. C.; Mirkin, C. A. *J. Am. Chem. Soc.* **2005**, *127*, 5312.
(7) Millstone, J. E.; Hurst, S. J.; Métraux, G. S.; Cutler, J. I.; Mirkin, C. A. *Small* **2009**, *5*, 646.
(8) Hurst, S. J.; Payne, E. K.; Qin, L.; Mirkin, C. A. *Angew. Chem., Int. Ed.* **2006**, *45*, 2672.
(9) Tao, A. R.; Habas, S.; Yang, P. *Small* **2008**, *4*, 310.
(10) Jones, M. R.; Osberg, K. D.; Macfarlane, R. J.; Langille, M. R.; Mirkin, C. A. *Chem. Rev.* **2011**, *111*, 3736.
(11) Zhou, Z.-Y.; Tian, N.; Li, J.-T.; Broadwell, I.; Sun, S.-G. *Chem. Soc. Rev.* **2011**, *40*, 4167.
(12) Somorjai, G. A.; Frei, H.; Park, J. Y. *J. Am. Chem. Soc.* **2009**, *131*, 16589.
(13) Tian, N.; Zhou, Z.-Y.; Sun, S.-G.; Ding, Y.; Wang, Z. L. *Science* **2007**, *316*, 732.
(14) Giljohann, D. A.; Seferos, D. S.; Daniel, W. L.; Massich, M. D.; Patel, P. C.; Mirkin, C. A. *Angew. Chem., Int. Ed.* **2010**, *49*, 3280.
(15) Langille, M. R.; Zhang, J.; Mirkin, C. A. *Angew. Chem., Int. Ed.* **2011**, *50*, 3543.
(16) Langille, M. R.; Zhang, J.; Personick, M. L.; Li, S.; Mirkin, C. A. *Science* **2012**, *337*, 954.
(17) Jin, R.; Cao, Y.; Mirkin, C. A.; Kelly, K. L.; Schatz, G. C.; Zheng, J. G. *Science* **2001**, *294*, 1901.
(18) Jin, R.; Cao, Y. C.; Hao, E.; Métraux, G. S.; Schatz, G. C.; Mirkin, C. A. *Nature* **2003**, *425*, 487.
(19) Zheng, X.; Zhao, X.; Guo, D.; Tang, B.; Xu, S.; Zhao, B.; Xu, W.; Lombardi, J. R. *Langmuir* **2009**, *25*, 3802.
(20) Yu, T.; Kim, D. Y.; Zhang, H.; Xia, Y. *Angew. Chem., Int. Ed.* **2011**, *50*, 2773.
(21) Wiley, B. J.; Xiong, Y.; Li, Z.-Y.; Yin, Y.; Xia, Y. *Nano Lett.* **2006**, *6*, 765.
(22) Xia, X.; Zeng, J.; McDearmon, B.; Zheng, Y.; Li, Q.; Xia, Y. *Angew. Chem., Int. Ed.* **2011**, *50*, 12542.
(23) Wiley, B.; Herricks, T.; Sun, Y.; Xia, Y. *Nano Lett.* **2004**, *4*, 1733.
(24) Tran, T. T.; Lu, X. *J. Phys. Chem. C* **2011**, *115*, 3638.
(25) Sau, T. K.; Rogach, A. L. *Adv. Mater.* **2010**, *22*, 1781.
(26) Pietrobon, B.; Kitaev, V. *Chem. Mater.* **2008**, *20*, 5186.
(27) Niu, W.; Zheng, S.; Wang, D.; Liu, X.; Li, H.; Han, S.; Chen, J.; Tang, Z.; Xu, G. *J. Am. Chem. Soc.* **2009**, *131*, 697.
(28) Jin, M.; Zhang, H.; Xie, Z.; Xia, Y. *Angew. Chem., Int. Ed.* **2011**, *50*, 7850.
(29) DeSantis, C. J.; Peverly, A. A.; Peters, D. G.; Skrabalak, S. E. *Nano Lett.* **2011**, *11*, 2164.
(30) Personick, M. L.; Langille, M. R.; Zhang, J.; Wu, J.; Li, S.; Mirkin, C. A. *Small* **2013**, *9*, 1947.
(31) Xue, C.; Métraux, G. S.; Millstone, J. E.; Mirkin, C. A. *J. Am. Chem. Soc.* **2008**, *130*, 8337.
(32) Xue, C.; Millstone, J. E.; Li, S.; Mirkin, C. A. *Angew. Chem., Int. Ed.* **2007**, *46*, 8436.
(33) Zhang, J.; Langille, M. R.; Mirkin, C. A. *J. Am. Chem. Soc.* **2010**, *132*, 12502.
(34) Xue, C.; Mirkin, C. A. *Angew. Chem., Int. Ed.* **2007**, *46*, 2036.
(35) Zhang, J.; Langille, M. R.; Mirkin, C. A. *Nano Lett.* **2011**, *11*, 2495.
(36) Langille, M. R.; Personick, M. L.; Zhang, J.; Mirkin, C. A. *J. Am. Chem. Soc.* **2011**, *133*, 10414.
(37) Zhang, J.; Li, S.; Wu, J.; Schatz, G. C.; Mirkin, C. A. *Angew. Chem., Int. Ed.* **2009**, *48*, 7787.
(38) Langille, M. R.; Personick, M. L.; Zhang, J.; Mirkin, C. A. *J. Am. Chem. Soc.* **2012**, *134*, 14542.
(39) Personick, M. L.; Langille, M. R.; Zhang, J.; Mirkin, C. A. *Nano Lett.* **2011**, *11*, 3394.
(40) Zhang, J.; Langille, M. R.; Personick, M. L.; Zhang, K.; Li, S.; Mirkin, C. A. *J. Am. Chem. Soc.* **2010**, *132*, 14012.
(41) Kim, F.; Connor, S.; Song, H.; Kuykendall, T.; Yang, P. *Angew. Chem., Int. Ed.* **2004**, *43*, 3673.
(42) Ming, T.; Feng, W.; Tang, Q.; Wang, F.; Sun, L.; Wang, J.; Yan, C. *J. Am. Chem. Soc.* **2009**, *131*, 16350.
(43) Carbó-Argibay, E.; Rodríguez-González, B.; Gómez-Graña, S.; Guerrero-Martínez, A.; Pastoriza-Santos, I.; Pérez-Juste, J.; Liz-Marzán, L. M. *Angew. Chem., Int. Ed.* **2010**, *49*, 9397.
(44) Jana, N. R.; Gearheart, L.; Murphy, C. J. *J. Phys. Chem. B* **2001**, *105*, 4065.
(45) Nikoobakht, B.; El-Sayed, M. A. *Chem. Mater.* **2003**, *15*, 1957.
(46) Sau, T. K.; Murphy, C. J. *J. Am. Chem. Soc.* **2004**, *126*, 8648.
(47) Sun, Y.; Xia, Y. *Science* **2002**, *298*, 2176.
(48) Grzelczak, M.; Pérez-Juste, J.; Mulvaney, P.; Liz-Marzán, L. M. *Chem. Soc. Rev.* **2008**, *37*, 1783.
(49) Kumar, P. S.; Pastoriza-Santos, I.; Rodríguez-González, B.; García de Abajo, F. J.; Liz-Marzán, L. M. *Nanotechnology* **2008**, *19*, 015606.
(50) Li, J.; Wang, L.; Liu, L.; Guo, L.; Han, X.; Zhang, Z. *Chem. Commun.* **2010**, *46*, 5109.
(51) Ma, Y.; Kuang, Q.; Jiang, Z.; Xie, Z.; Huang, R.; Zheng, L. *Angew. Chem., Int. Ed.* **2008**, *47*, 8901.
(52) Yu, Y.; Zhang, Q.; Lu, X.; Lee, J. Y. *J. Phys. Chem. C* **2010**, *114*, 11119.
(53) Personick, M. L.; Langille, M. R.; Zhang, J.; Harris, N.; Schatz, G. C.; Mirkin, C. A. *J. Am. Chem. Soc.* **2011**, *133*, 6170.
(54) Personick, M. L.; Langille, M. R.; Wu, J.; Mirkin, C. A. *J. Am. Chem. Soc.* **2013**, *135*, 3800.

(55) Elechiguerra, J. L.; Reyes-Gasga, J.; Yacamán, M. J. *J. Mater. Chem.* **2006**, *16*, 3906.
(56) Lofton, C.; Sigmund, W. *Adv. Funct. Mater.* **2005**, *15*, 1197.
(57) Wang, Z. L. *J. Phys. Chem. B* **2000**, *104*, 1153.
(58) Kim, D.; Heo, J.; Kim, M.; Lee, Y. W.; Han, S. W. *Chem. Phys. Lett.* **2009**, *468*, 245.
(59) Xiang, Y.; Wu, X.; Liu, D.; Feng, L.; Zhang, K.; Chu, W.; Zhou, W.; Xie, S. *J. Phys. Chem. C* **2008**, *112*, 3203.
(60) Eguchi, M.; Mitsui, D.; Wu, H.-L.; Sato, R.; Teranishi, T. *Langmuir* **2012**, *28*, 9021.
(61) Millstone, J. E.; Métraux, G. S.; Mirkin, C. A. *Adv. Funct. Mater.* **2006**, *16*, 1209.
(62) Millstone, J. E.; Wei, W.; Jones, M. R.; Yoo, H.; Mirkin, C. A. *Nano Lett.* **2008**, *8*, 2526.
(63) Liu, M.; Guyot-Sionnest, P. *J. Phys. Chem. B* **2005**, *109*, 22192.
(64) Zhang, H.; Jin, M.; Xia, Y. *Angew. Chem., Int. Ed.* **2012**, *51*, 7656.
(65) Jana, N. R.; Gearheart, L.; Murphy, C. J. *Adv. Mater.* **2001**, *13*, 1389.
(66) Gole, A.; Murphy, C. J. *Chem. Mater.* **2004**, *16*, 3633.
(67) Zhang, Q.; Xie, J.; Yu, Y.; Yang, J.; Lee, J. Y. *Small* **2010**, *6*, 523.
(68) Wu, H.-L.; Kuo, C.-H.; Huang, M. H. *Langmuir* **2010**, *26*, 12307.
(69) Bullen, C.; Zijlstra, P.; Bakker, E.; Gu, M.; Raston, C. *Cryst. Growth Des.* **2011**, *11*, 3375.
(70) Bard, A. J.; Parsons, R.; Jordan, J. *Standard Potentials in Aqueous Solution*; Marcel Dekker: New York, 1985.
(71) Brown, L.; Holme, T. *Chemistry for Engineering Students*; Brooks/Cole: Belmont, 2011.
(72) Magnussen, O. M. *Chem. Rev.* **2002**, *102*, 679.
(73) Herrero, E.; Buller, L. J.; Abruña, H. D. *Chem. Rev.* **2001**, *101*, 1897.
(74) Oviedo, O. A.; Negre, C. F. A.; Mariscal, M. M.; Sánchez, C. G.; Leiva, E. P. M. *Electrochem. Commun.* **2012**, *16*, 1.
(75) Michalitsch, R.; Palmer, B. J.; Laibinis, P. E. *Langmuir* **2000**, *16*, 6533.
(76) Lee, J.; Oh, I.; Hwang, S.; Kwak, J. *Langmuir* **2002**, *18*, 8025.
(77) Iski, E. V.; El-Kouedi, M.; Calderon, C.; Wang, F.; Bellisario, D. O.; Ye, T.; Sykes, E. C. H. *Electrochim. Acta* **2011**, *56*, 1652.
(78) Michalitsch, R.; Laibinis, P. E. *Angew. Chem., Int. Ed.* **2001**, *40*, 941.
(79) Pérez-Juste, J.; Liz-Marzán, L. M.; Carnie, S.; Chan, D. Y. C.; Mulvaney, P. *Adv. Funct. Mater.* **2004**, *14*, 571.
(80) Rodríguez-Fernández, J.; Pérez-Juste, J.; Mulvaney, P.; Liz-Marzán, L. M. *J. Phys. Chem. B* **2005**, *109*, 14257.
(81) Sánchez, C. G.; Del Pópolo, M. G.; Leiva, E. P. M. *Surf. Sci.* **1999**, *421*, 59.
(82) Chierchie, T.; Mayer, C. *Electrochim. Acta* **1988**, *33*, 341.
(83) Zhu, C.; Zeng, J.; Lu, P.; Liu, J.; Gu, Z.; Xia, Y. *Chem. Eur. J.* **2013**, *19*, 5127.
(84) Lindstrom, C. D.; Zhu, X.-Y. *Chem. Rev.* **2006**, *106*, 4281.